JOC The Journal of Organic Chemistry

ARTICLE

pubs.acs.org/joc

DABCO as a Dynamic Hinge between Cofacial Porphyrin Panels and Its Tumbling inside a Supramolecular Cavity

Soumen K. Samanta,[†] Debabrata Samanta,[†] Jan W. Bats,[‡] and Michael Schmittel*[,†]

[†]Center for Micro- and Nanochemistry and Engineering, Organische Chemie I, Adolf-Reichwein Strasse, Universität Siegen, D-57068 Siegen, Germany

[‡]Institut für Organische Chemie und Chemische Biologie, Johann Wolfgang Goethe-Universität, Max-von-Laue-Strasse 7, D-60438 Frankfurt am Main, Germany

Supporting Information

ABSTRACT:

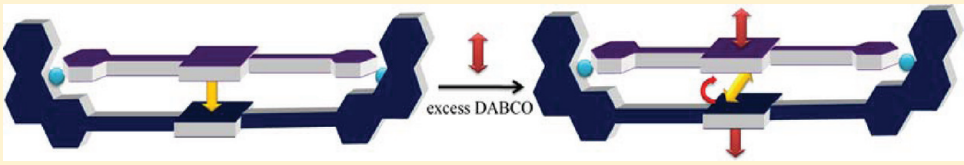

The heteroleptic supramolecular double-decker porphyrin **1** was synthesized with DABCO as a guest between two cofacial porphyrin units as characterized by ^{1}H NMR and ESI-MS. While DABCO is not seen to tumble inside the cavity, even at higher temperatures (80 °C), such motion was triggered upon addition of various coordinating ligands (quinuclidine, 4-bromopyridine, or excess of DABCO). Different stoichiometric amounts were needed depending on the n donor quality of the added ligands to initiate tumbling of the "inside" DABCO. As demonstrated in an example with excess DABCO, the tumbling was stopped by lowering the temperature to −50 °C.

INTRODUCTION

Transformation of energy into motion plays an important role in both real-world machinery as well as (bio)molecular machines.[1] As a consequence, large-amplitude motion at the molecular level, initiated by external stimuli, has garnered major attention in recent years.[2] Molecular motion may take place either in a directed or undirected fashion, resulting in either (pseudo)linear or rotational movement. Many molecular nanoswitches—a subcategory of nanomachines—operate with large-amplitude linear drive, as seen, for example, in rotaxanes and catenanes.[1,3] Other molecular nanoswitches follow a different design: the molecular parts rotate about a hinge, the requirements for which are mostly 2-fold: (i) the hinge should impart a very low barrier of rotation to the ensemble, and (ii) it should allow for convenient synthetic accessibility. While in most cases the molecular switch is operating at a covalent hinge or axle,[4,5] in a few examples a dynamic hinge is used.[6] Profitably, utilization of a dynamic hinge allows to self-assemble all parts of a nanoswitch in a final supramolecular process.

In the context of our ongoing work toward nanoswitches (Figure 1), we herein present a study on the usefulness of DABCO as a dynamic hinge between two porphyrin panels. Clearly, the practicability of a dynamic DABCO hinge ("inside" DABCO) would be jeopardized if excess DABCO, i.e., free DABCO, exchanged with the "inside" DABCO or if it destroyed the supramolecular ensemble. In addition, free DABCO may actuate the "inside" DABCO through the zinc(II)−porphyrin plane.[7] Thus, to understand the dynamic and thermodynamic

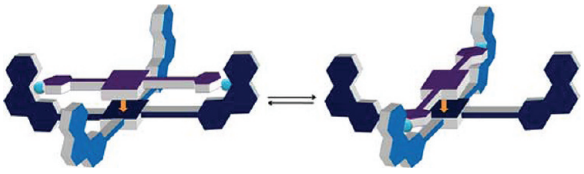

Figure 1. Schematic diagram of a molecular switch operating between two stations.

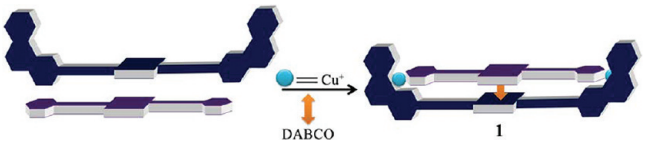

Figure 2. Cartoon representation of the porphyrin heterodimer **1**.

implications of a dynamic DABCO-hinged nanoswitch, we decided to study the supramolecular heteroleptic double-decker porphyrin **1** with DABCO as a guest (Figure 2). Using this complex, different stimuli such as DABCO, quinuclidine, and pyridine derivatives were studied at different concentrations to evaluate the dynamics of the "inside" DABCO.

Received: June 18, 2011
Published: August 24, 2011

Chart 1. Ligands Used in This Study along with Their Cartoon Representations

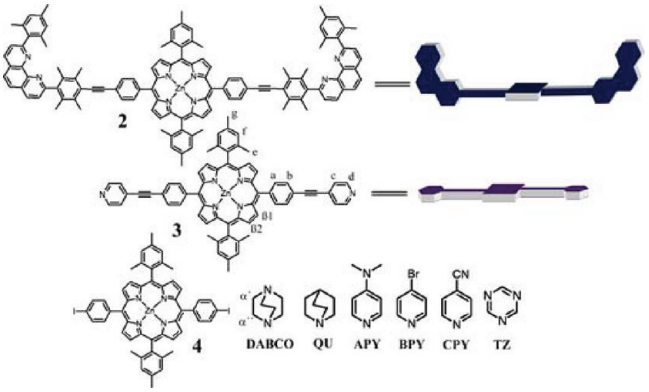

The growing interest in the dynamics of guest molecules inside a supramolecular cavity has resulted in fascinating new molecular entities with potential nanomechanical applications.[8] If the rotation of a molecule or part of it can be triggered and controlled, it may act as a rotator. In most known cases, the motion of the guest is only possible along a given axis.[9] However, there are other examples[10] where tumbling was induced by temperature and controlled by the shape and size of the guest. According to our knowledge, there are no examples in the literature where the tumbling motion is initiated only by external additives as triggers. Herein, we thus like to present the preparation and chemomechanical actuation[11] of the DABCO-bridged supramolecular double-decker porphyrin **1**, in which the tumbling motion of DABCO is induced by chemical input.

As a basis for the heteroleptic four-component assembly **1**, we have chosen ligands **2** and **3** (Chart 1). Because DABCO alone cannot control heteroleptic aggregation of **2** and **3**, the two ligands were anchored together by the HETPYP approach,[12] while DABCO was sandwiched between the two zinc(II) porphyrins. The HETPYP approach assures the formation of a heteroleptic copper(I) or silver(I) complex with one sterically shielded phenanthroline and pyridine(s) as ligands.[12]

RESULTS AND DISCUSSION

Preparation of the Ligands. The ligands used in the present study are depicted in Chart 1. Compound **2** has been described previously.[7]

Compound **3** was prepared in 59% yield by reacting zinc(II)−5, 15-bis-(4-iodophenyl)-10,20-(2,4,6-trimethylphenyl)porphyrin with 4-ethynylpyridine. Single crystals of **3** suitable for X-ray diffraction were grown by slow evaporation of a chloroform and toluene mixture (3:1). The X-ray analysis reveals that compound **3** crystallizes in the monoclinic space group $P21/c$. The crystal structure shows the presence of four molecules of **3** in the unit cell. Each zinc(II) ion exhibits hexacoordination with a distorted octahedral geometry with four nitrogen atoms of the porphyrin moiety (Zn1···N1 = 2.054 Å, Zn1···N2 = 2.075 Å, Zn1···N3 = 1.997 Å, Zn1···N4 = 2.113 Å) and two pyridine nitrogens from two additional ligands **3** (Zn1···N5 = 2.345 Å and Zn1···N6 = 2.328 Å). The molecule self-assembles via axial interaction of the pyridine units to the zinc(II) center of the porphyrin to form an infinite 2D rhombus grid network (Figure 3). An interesting feature of the structure is that each of

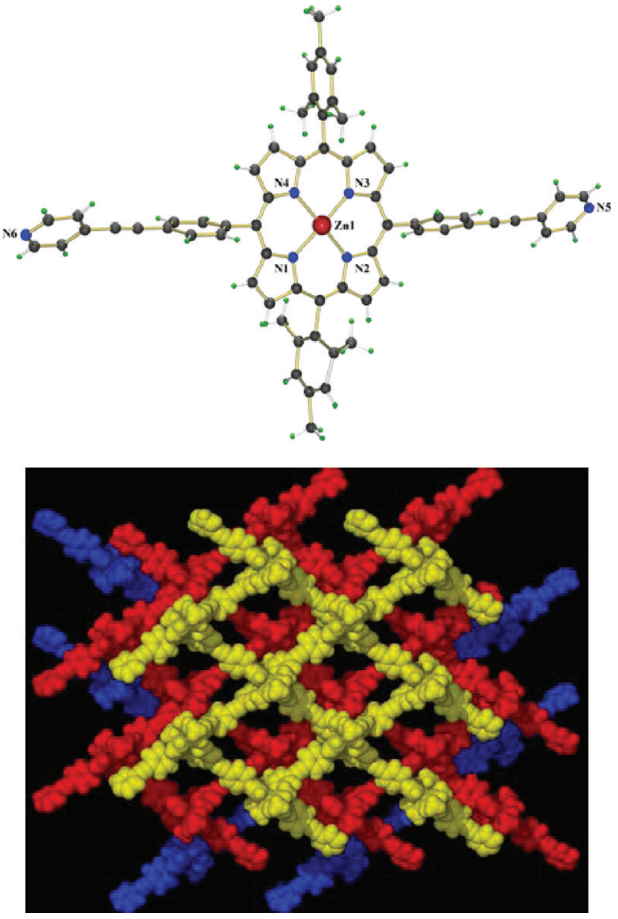

Figure 3. Crystal structure of compound **3** (top) and packing of the compound (bottom).

the grid networks is lying on top of each other to form a 3D framework generating a one-dimensional channel passing through the crystallographic b axis. These channels are not empty but occupied by toluene guest molecules. The latter, however, are much disordered possibly the origin of the poor quality of the crystal. Several attempts to grow better single crystals in chloroform/toluene (3:1) as well as trying different solvent mixtures proved unsuccessful. The layered structure is stabilized by strong C−H···π interactions (2.85 Å) between the mesityl rings and phenyl H atoms of the adjacent layer. Another important CH···π interaction (2.80 Å) that stabilizes the layer structure is seen between the methyl group of the mesityl ring and the porphyrin β H atoms.

Preparation and Characterization of 1. In a first set of experiments, an equimolar mixture of **2** and **3** was treated with 2 equiv of $[Cu(CH_3CN)_4]PF_6$ in dry $CHCl_3$/DCM (1:1) for 3 h at 60 °C to prepare $[Cu_2(\mathbf{2})(\mathbf{3})](PF_6)_2$. Revealingly, the ^{1}H NMR was characterized by broad resonances and, moreover, did not show the characteristic upfield shift of the pyridyl protons to ca. 6.5−7.2 ppm as would be diagnostic for a HETPYP complex. Possibly, the axial interaction of the zinc(II) porphyrin with pyridine competes with the targeted HETPYP interaction as both are thermodynamically competitive. However, when 1.0 equiv of DABCO was added to the reaction mixture, the porphyrin double decker **1** formed in a clean manner (Figure 4). Two sharp singlets appeared at −4.54 and

dx.doi.org/10.1021/jo201252q | J. Org. Chem. 2011, 76, 7466–7473

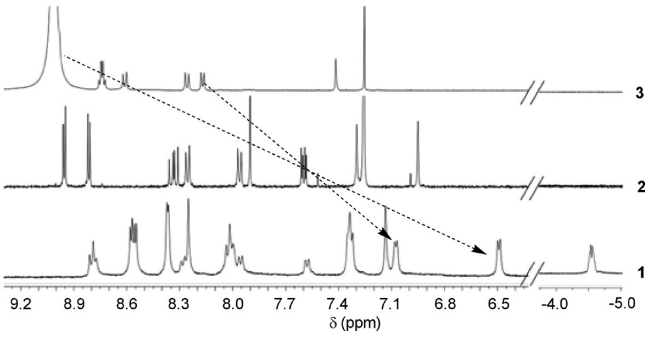

Figure 4. Partial ^{1}H NMR (400 MHz, 298 K) spectra of **1** (CD_2Cl_2/$CDCl_3$ = 9:1), **2** ($CDCl_3$) and **3** ($CDCl_3$/TFA = 99.5:0.5). A part of the spectrum of **3** is covered by TFA (δ = 9.02 ppm).

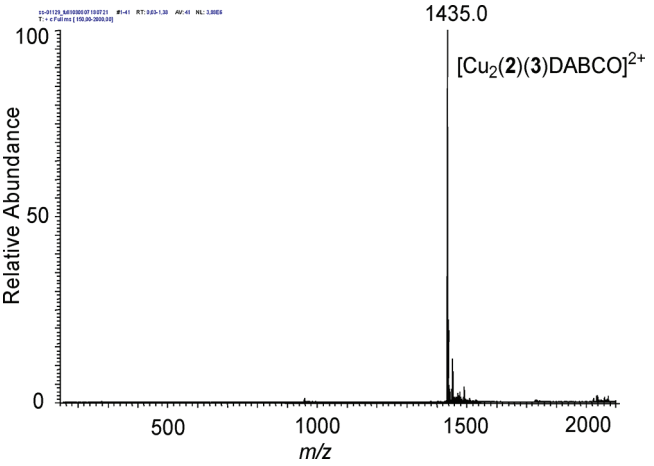

Figure 5. ESI-MS spectrum of **1** in CH_2Cl_2.

−4.57 ppm in the ^{1}H NMR being diagnostic for DABCO methylene protons in a porphyrin−DABCO sandwich complex,[7,13] along with characteristic peaks for the HETPYP complex. For example, the d and c protons of the pyridine units appeared at 6.49 and 7.08 ppm, respectively. Unlike in the HETPHEN and HETTAP complexation motif,[14] the mesityl protons of the phenanthroline units show the same chemical shift before and after HETPYP complexation and are thus not diagnostically relevant. The spectrum was analyzed by ^{1}H−^{1}H COSY corroborating the structure. Four different sets of porphyrin β protons were observed in the ^{1}H NMR attesting the geometrically unsymmetrical environment. Finally, ^{1}H DOSY proved **1** (2.71 mM) to be a single species in solution.

The four-component complex **1** = $[Cu_2(\mathbf{2})(\mathbf{3})(DABCO)](PF_6)_2$ was furthermore characterized through its very clean ESI-MS spectrum (Figure 5). A peak at 1435.0 Da corresponding to the doubly charged species, $[Cu_2(\mathbf{2})(\mathbf{3})(DABCO)]^{2+}$, is diagnostic of complex **1** that has lost two PF_6^- counteranions. Accordingly, each copper(I) ion has only three coordination sites filled, possibly in a trigonal arrangement, which is very rare.[15] In this binding situation the phenanthroline provides more shielding to the pyridine protons (6.49 and 7.08 ppm) (Figure 4) than in the case of a tetrahedral arrangement (7.39 and 7.55 ppm).[12] Complex **1** was additionally characterized by ^{13}C NMR and elemental analysis. While it is difficult for copper(I) to tolerate a three-ligand coordination scenario, silver(I) can readily

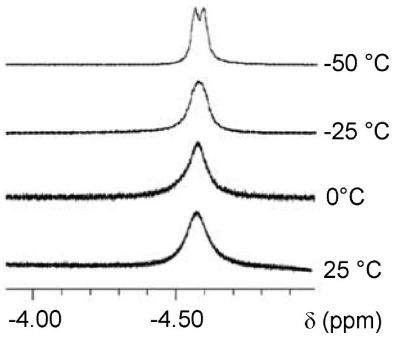

Figure 6. Low-temperature ^{1}H NMR of the mixture **1**/DABCO = 1:4.

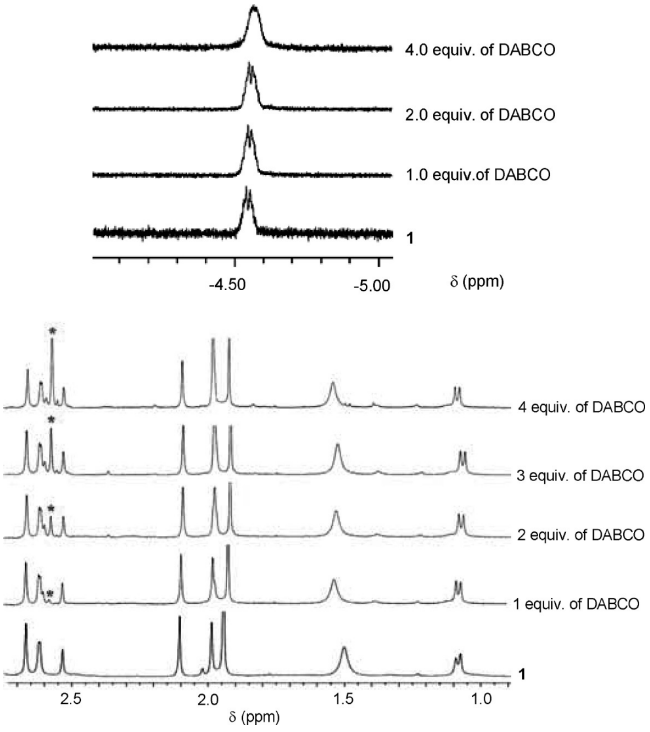

Figure 7. ^{1}H NMR titration of **1** with DABCO in CD_2Cl_2 at 298 K. Top: Negative region of the spectra. Bottom: Aliphatic region of the spectra. *Peaks of "free" DABCO.

adjust with coordination numbers from 2 to 6. Hence, the analogous structure $[Ag_2(\mathbf{2})(\mathbf{3})(DABCO)]^{2+}$ was prepared using silver(I) as characterized by ^{1}H NMR and ESI-MS (see the Supporting Information).

Actuation of DABCO inside the Cavity. To investigate the dynamic behavior of DABCO inside the cavity, **1** was titrated with excess amounts of DABCO (Figure 6 and 7). Upon addition of 1 equiv of DABCO to **1**, the two singlets of the DABCO methylene protons (α', α'') remained at −4.54 and −4.57 ppm, while a new peak emerged at 2.58 ppm corresponding to free DABCO[16] in solution. Obviously, as judged by the lack of coalescence, at this ratio there is no exchange between "inside" and free DABCO. Upon addition of further 3 equiv of DABCO, the two singlets of the encapsulated DABCO coalesced into a broad singlet at −4.55 ppm, but still no exchange with the added DABCO was detected. Possibly, the kinetic stability is due to the steric crowding provided by the aryl groups of both porphyrin

dx.doi.org/10.1021/jo201252q |J. Org. Chem. 2011, 76, 7466–7473

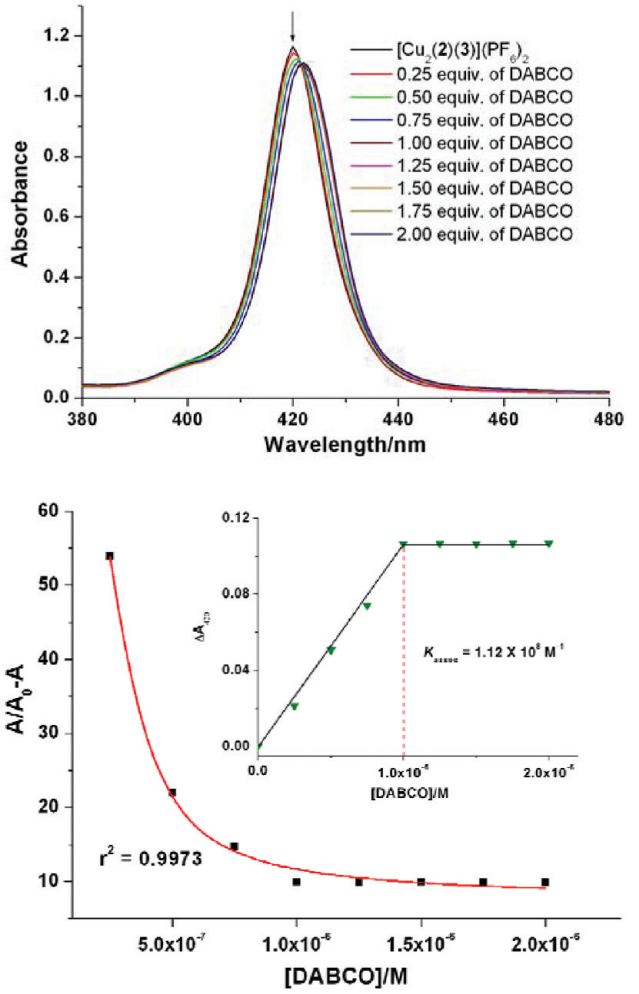

Figure 8. Top: UV−vis titration of $[Cu_2(\mathbf{2})(\mathbf{3})](PF_6)_2$ (1.0×10^{-6} M) with DABCO (1.0×10^{-4} M) in CH_2Cl_2 at 298 K. Bottom: Fitting curve: ΔAbs was monitored at 420 nm. (Inset: plot of ΔA_{420} vs [DABCO]).

units. An MM+ computed structure of **1** (see the Supporting Information, Figure S21) showed that DABCO is rather crowdedly surrounded by the *meso*-aryl groups of both porphyrin panels, thus blocking any easy escape from the cavity.

The firm binding of DABCO in **1** may also be addressed from a thermochemical point of view (Figure 8). Upon addition of 1 equiv of DABCO to the reaction mixture of **2**, **3**, and Cu^+ (1:1:2), the UV−vis spectrum showed a bathochromic shift of the Soret and Q-bands, whereas with more than 1 equiv of DABCO the absorption spectrum did not exhibit any further changes, suggesting that there is no exchange between free and "inside" DABCO in solution. From this spectrophotometric titration,[17] the association constant K_{assoc} of DABCO to "$[Cu_2(\mathbf{2})(\mathbf{3})]^{2+}$" was determined. As "$[Cu_2(\mathbf{2})(\mathbf{3})]^{2+}$" is an equilibrating mixture of $[Cu_2(\mathbf{2})(\mathbf{3})]^{2+}$ and pyridine−zinc(II) porphyrin complexes, the found association constant of $(1.12 \pm 0.22) \times 10^8$ M^{-1} (log K_{assoc} = 8.05 ± 0.68) is not well-defined for $[Cu_2(\mathbf{2})(\mathbf{3})(DABCO)]^{2+}$. Nevertheless, the large log K_{assoc} points to a high thermodynamic stabilization[18] of **1** through the strong binding of DABCO inside the cavity. Thus, there are both good thermochemical and kinetic arguments against exchange of free and "inside" DABCO.

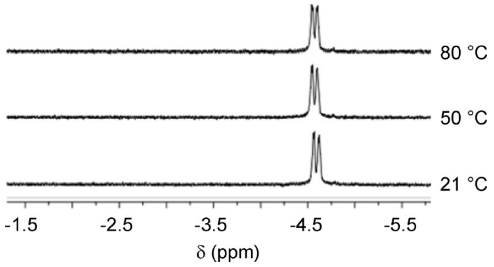

Figure 9. High-temperature VT-NMR experiment of **1**.

Further insight was obtained upon probing the mixture (**1**/DABCO = 1:4) at low temperature (Figure 6, right). The broad signal (δ = −4.55 ppm) became sharp when lowering the temperature down to −25 °C and split into two singlets at −50 °C. Such a finding advocates a model that, at room temperature in the presence of excess DABCO, the "inside" DABCO not only rotates about the N−N axis but tumbles[9b,c,10] inside the cavity. Such a process leads to an exchange of the methylene protons inside the unsymmetric cavity entailing their coalescence into a broad signal. Upon cooling to −50 °C, tumbling is frozen and the DABCO methylene protons experience the unsymmetrical environment resulting in a splitting of the broad peak. The kinetics of this process is analyzed using the program WinDNMR[19] through simulation of the experimental spectra (see the Supporting Information, Figure S18), providing rate constants at various temperatures. Activation parameters are determined from an Eyring plot to be $\Delta H^{\ddagger} = 48.7 \pm 0.23$ kJ mol^{-1} and $\Delta S^{\ddagger} = 8.9 \pm 0.90$ J mol^{-1} K^{-1}. The slightly positive activation entropy suggests that in the transition state the negative entropic contribution of the **1**·DABCO association is well compensated by the positive contribution of the DABCO tumbling. At the coalescence temperature T_c = −25 °C, the activation barrier was determined as $\Delta G^{\ddagger}$ = 46.1 kJ mol^{-1}. Using the activation barrier, the corresponding association constant (K_{assoc}) of DABCO to $[Cu_2(\mathbf{2})(\mathbf{3})](PF_6)_2$ is determined to 1.2×10^8 M^{-1}, which is in good agreement with the $K_{assoc} = 1.12 \times 10^8$ M^{-1} obtained from UV−vis titration (vide supra).

Upon addition of excess of DABCO to **1**, free DABCO molecules attack the zinc(II) porphyrin from outside of the cavity, thus labilizing the DABCO within the cavity ("inside" DABCO). Generally, the zinc(II) porphyrin cannot strongly embrace a DABCO molecule in its axial position while coordinating to a second DABCO.[7,20] Because of the high association constant of "inside" DABCO and its effective kinetic shielding, free DABCO only labilizes the "inside" DABCO at elevated amounts, but does not exchange with it (as observed from the constant chemical shift, δ = −4.55 ppm).

When a sample of **1** was heated at elevated temperature (80 °C), the two singlets of DABCO did not coalesce into a broad signal (Figure 9). This observation excludes any tumbling motion[10] of DABCO at room temperature as well as at elevated temperature in the absence of excess DABCO. Only rotation about the N····N axis of DABCO seems to happen, which exchanges the six protons in the α' position and the six protons in the α'' position to furnish two singlets.

Tumbling of DABCO in the Presence of Other Actuators. The utility of added external DABCO to effect a tumbling motion of the DABCO inside the double-decker pophyrin raised the question of whether related molecules like quinuclidine (QU) or derivatives of pyridine would equally operate as actuators. Both are

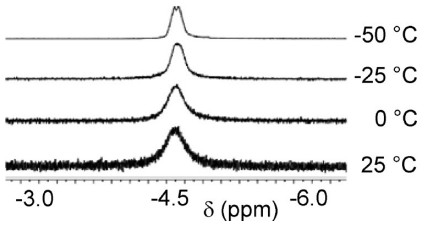

Figure 10. Low-temperature VT-NMR of the mixture **1**/QU = 1:4.

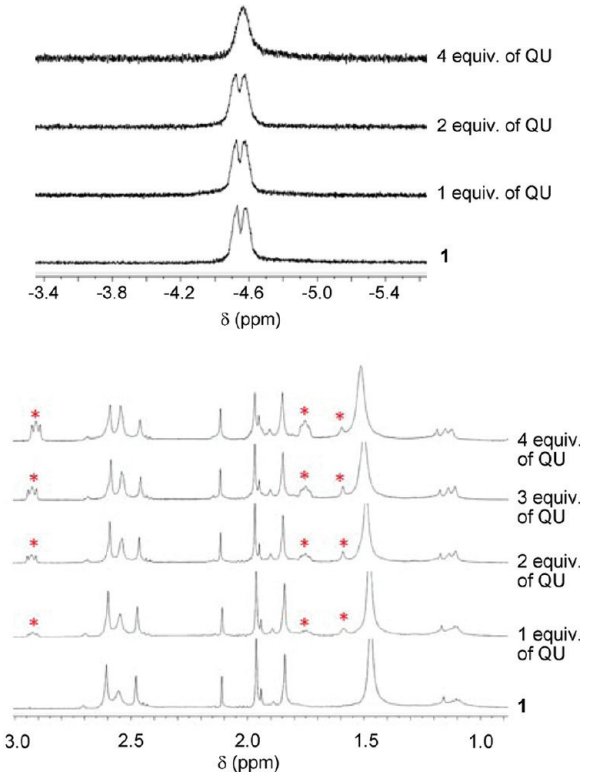

Figure 11. ^{1}H NMR titration of **1** with quinuclidine (QU) in CD_2Cl_2 at 298 K. Top: Negative region of the spectra. Bottom: Aliphatic region of the spectra. *Peaks of free QU.

well-known to coordinate to zinc porphyrins, such as the simple reference compound **4**.[13,21] Using UV−vis titrations, their association constants to **4** were determined as 1.3×10^5 M^{-1} for QU and as 3.0×10^4 M^{-1} for 4-bromopyridine (BPY).[17] When **4** was titrated with 1 equiv of QU, three sharp signals were observed in the ^{1}H NMR at −2.68, −0.40, and 0.29 ppm corresponding to the binary complex **4**·QU (see the Supporting Information). Importantly, upon addition of 0.25 equiv of excess of QU the peaks were shifted downfield pointing to a rapid equilibration between "bound" and free quinuclidine in solution. The peaks were further shifted downfield upon addition of further excess of QU.

In an another experiment, the addition of 0.5 equiv of DABCO to **4** furnished the expected sandwich complex $(\mathbf{4})_2$·DABCO (δ = −4.47 ppm for CH_2^{DABCO}), which broke down immediately upon addition of 0.25 equiv of QU. A peak at −2.64 ppm corresponding to the **4**·QU complex and a broad peak at −4.25 ppm (slightly downfield shifted) pointed to a rapid equilibrium between $(\mathbf{4})_2$·DABCO, and **4**·DABCO. At 0.5 equiv of quinuclidine, the two binary complexes **4**·QU and **4**·DABCO were detected.

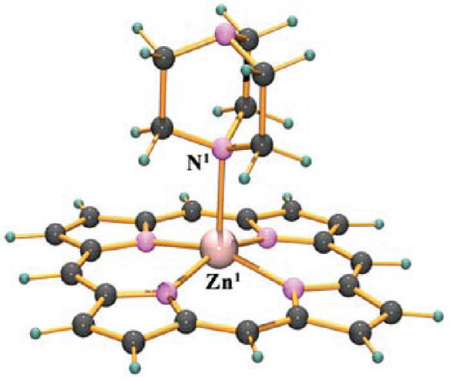

Figure 12. Molecular structure of **4**·DABCO (Zn1−N1 = 2.322 Å) calculated with Gaussian03 at the B3LYP/6-31G (d) level using LANL2DZ ECP for zinc.

When 1 equiv of QU was added to **1**, two sharp DABCO singlets at −4.54 and −4.57 ppm were observed along with peaks at 2.95, 1.73, and 1.53 ppm corresponding to free QU in solution indicating that no liberation of the "inside" DABCO took place. Upon addition of another 2 equiv of QU, the two singlets at δ = −4.54 and −4.57 ppm started to coalesce and finally merged into a broad singlet (δ = −4.55 ppm) with a further 1 equiv of QU added (Figures 10 and 11). Even at 8 equiv of QU, the broad peak of the DABCO protons remained at −4.55 ppm (see the Supporting Information). No peak for QU was observed in the negative region of NMR spectra, as QU is apparently endergonically bound at the outside of **1**. When a mixture of **1** and QU (1:4) was probed at low temperature, the broad peak split into two singlets at −50 °C, indicating the freezing of the tumbling motion of the "inside" DABCO. Thus, we conclude that both QU and DABCO can effect tumbling of the "inside" DABCO without liberating it from the cavity.

A similar behavior was noticed with 4-bromopyridine (BPY) as actuator (see Supporting Information). Coalescence of the two DABCO singlets required the addition of 9 equiv of BPY. BPY is a much weaker n donor than DABCO and QU, which readily explains the necessity to use a larger excess of this pyridine to labilize the "inside" DABCO.

DFT Computations. DFT computations using the B3LYP/6-31G (d) method were used to study the ternary complexes. Computationally the binding strength of DABCO to **4** (Figure 12) was determined as 7.0×10^6 M^{-1}, with the experimental value being 1.5×10^5 M^{-1} (in DCM). While the computed data overestimate the association constants, they are still useful to estimate the DABCO—zinc(II) binding strength in ternary complexes as the latter cannot be observed in the experiment due to their endergonic formation. Thus, using the same method, the DABCO—zinc(II) binding strength was computed in ternary complexes and was found to be 0.2×10^2 M^{-1} for **4**·$(DABCO)_2$ and 4.0×10^2 M^{-1} for **4**·(DABCO)-(BPY). The lower numbers indicate that the DABCO−zinc(II) interaction is more reduced by addition of a second DABCO than by that of bromopyridine. In the series of **4**·(DABCO)-(pyridines), the computed trend (Table 1) is that the DABCO−zinc(II) interaction is more reduced in the series APY > BPY > CPY. This trend is well reflected in the amounts of pyridines needed to make DABCO tumble inside **1**. When **1** was titrated with 4-cyanopyridine (CPY), BPY, and 4-*N*,*N*-dimethylaminopyridine (APY) the following amounts were

dx.doi.org/10.1021/jo201252q |*J. Org. Chem.* 2011, 76, 7466–7473

Table 1. Zn−N_{DABCO} Bond Length and K_{assoc} in the Ternary Complex 4·(DABCO)(L) upon Addition of the Corresponding Ligands L as Calculated at the B3LYP/6-31G (d) Level Using LANL2DZ ECP for Zinc

L	equiv needed to make DABCO tumble in **1**	Zn−N_{DABCO} bond length in presence of other ligands (Å)	K_{assoc} /M^{-1} of DABCO in **4**·(DABCO)(**L**)
DABCO	4	2.956	0.20×10^2
QU	4	2.899	0.27×10^2
APY	6	2.845	0.38×10^2
BPY	9	2.688	4.0×10^2
CPY	20	2.490	5.9×10^4
		2.322	7.0×10^6

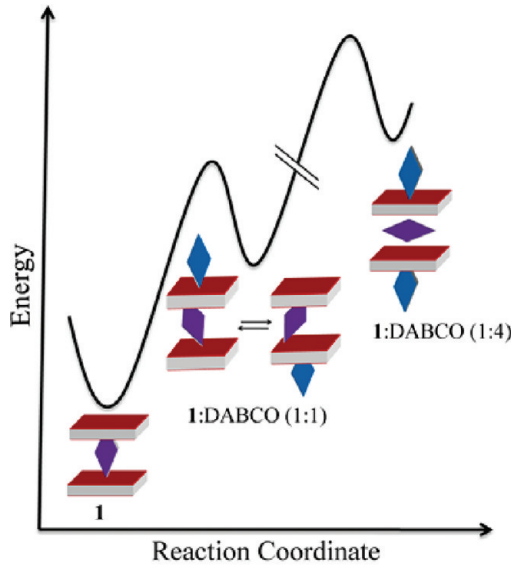

Figure 13. Proposed model for the tumbling motion of DABCO.

needed: 20, 9, and 6 equiv, respectively, reflecting the increased basicity and HOMO energy along CPY < BPY < APY.

In the experimental study, there is no evidence that **1** associates in any recognizable equilibrium amounts with any of the additives in solution (vide infra, Figure 13). Notably, a much weaker ligand, such as triazene (TZ), was not able to actuate the "inside" DABCO in **1**, not even in large excess (25 equiv). A model experiment showed that 3 equiv of triazene (TZ) could not even break up the model complex $(\mathbf{4})_2$·DABCO, attesting to the weakness of TZ in comparison with others (pyridines, quinuclidine, and DABCO).

Tumbling Motion. With all relevant data at hand the following picture emerges (Figure 13): In compound **1** the DABCO rotates about its N····N axis while being attached to the zinc centers of both porphyrin panels. Tumbling is not observed even at elevated temperatures (≤80 °C). Addition of 1 or 2 equiv of DABCO generates in an endergonic equilibrium the new complex **1**·DABCO through external coordination of DABCO. Since the "inside" DABCO remains strongly attached to one of the zinc centers in **1**·DABCO, no exchange of its α', α'' protons is seen. Only at larger amounts of DABCO (**1**/DABCO = 1/4) the complex $\mathbf{1}\cdot(\mathrm{DABCO})_2$ is formed in a highly endergonic step that allows for exchange of the α', α'' protons of the "inside" DABCO through a tumbling process.

Analogous to the situation with added DABCO, the other additives such as **L** = QU, APY, BPY and CPY trigger the "inside" DABCO to tumble through the formation of $\mathbf{1}\cdot(\mathbf{L})_2$. Both $\mathbf{1}\cdot(\mathbf{L})_2$ and $\mathbf{1}\cdot(\mathrm{DABCO})_2$, respectively, do form in a highly endergonic equilibrium with **1**, precluding experimental observation. To trigger tumbling as a chemomechanical action, the equivalents (amounts) of additives have thus to be adjusted in a way that they allow for a sufficient population of $\mathbf{1}\cdot(\mathbf{L})_2$. In $\mathbf{1}\cdot(\mathbf{L})_2$ the barrier of tumbling is so low that in **1** the α', α'' protons of DABCO exchange on the time scale of the NMR experiment.

SUMMARY

In conclusion, we have synthesized the supramolecular double-decker porphyrin **1** with DABCO as a rotating guest. The parent system does not show a tumbling motion, even at elevated temperature (80 °C). Addition of excess of various coordinating ligands (stimuli) to **1** actuate DABCO to undergo a tumbling motion at room temperature inside the cavity. Upon lowering the temperature to −50 °C the tumbling may be stopped. Depending on their donor properties, quite different amounts of the various stimuli are needed to make the DABCO molecule tumble. Such findings demonstrate that in absence of other coordinating ligands DABCO is kinetically and thermodynamically locked within the complex **1** even at elevated temperatures. The above results moreover provide a clue about the usefulness of DABCO in **1** as a dynamic hinge in molecular switches involving a bisphorphyrin hinge element. Further investigations will concentrate on molecular switches such as that presented in Figure 1 and whether the DABCO will be exchanged within the process of switching between two different stations.

EXPERIMENTAL SECTION

General Methods. Commercially available reagents were used without further purification. The solvents were dried with the appropriate desiccants and distilled prior to use. Silica gel 60 was used for column chromatography. ^{1}H and ^{13}C NMR spectra were recorded using the deuterated solvent as the lock and residual solvent as internal reference. The following abbreviations were utilized to describe NMR peak patterns: s = singlet, d = doublet, t = triplet. The following abbreviations were used to describe the peak patterns of IR spectra: s = sharp, m = medium, w = weak. The numbering of the carbon skeleton of the molecular formulas shown in the manuscript does not comply with the IUPAC nomenclature rules; it is only used for assignments of the NMR signal. Melting points are uncorrected. Binding constants were determined by UV−vis titrations in combination with the SPECFIT/32TM global analysis system.[17] The energy-minimized structures are calculated with Gaussian03 at the B3LYP/6-31G (d) level, using the LANL2DZ effective core potential for zinc.

Zinc(II)−5,15-bis[4-(4-ethynylpyridine)phenyl]-10,20-bis-[2,4,6-trimethylphenyl]porphyrin (3). Zinc(II)−5,15-bis-(4-iodophenyl)-10,20-bis-(2,4,6-trimethylphenyl)porphyrin (250 mg, 0.247 mmol) and 4-ethynylpyridine (50.9 mg, 0.494 mmol) were poured into a three-neck round-bottomed flask. $Pd(PPh_3)_4$ (28.5 mg, 24.7 μmol) was then added to the reaction mixture. Dry NEt_3 (10 mL) and dry DMF (30 mL) were added to the reaction mixture under N_2 atmosphere. The reaction mixture was then allowed to stir for 12 h at 90 °C. The reaction mixture was evaporated to dryness, dissolved in DCM (50 mL), and washed with water (3 × 50 mL). After drying over anhydrous Na_2SO_4, the solvent was

dx.doi.org/10.1021/jo201252q |J. Org. Chem. 2011, 76, 7466–7473

evaporated, and the residue was purified by column chromatography (SiO_2, DCM/MeOH = 99.5:0.5, R_f = 0.4). The compound was further purified by recrystallization from toluene/chloroform (3:1) mixture: yield 59%; mp >300 °C; ^{1}H NMR (400 MHz, $CDCl_3$/TFA = 99.5:0.5) δ = 1.93 (s, 12 H, e-H), 2.68 (s, 6 H, g-H), 7.42 (s, 4 H, f-H), 8.17 (d, ^3J = 6.6 Hz, 4 H, c-H), 8.26 (d, ^3J = 8.2 Hz, 4 H, a-H), 8.61 (d, ^3J = 8.2 Hz, 4 H, b-H), 8.72 (d, ^3J = 8.8 Hz, 4 H, β1-H), 8.73 (d, ^3J = 8.8 Hz, 4 H, β2-H), 9.03 (d, ^3J = 6.6 Hz, 4 H, d-H); ^{13}C NMR (100 MHz, $CDCl_3$/TFA = 99.5:0.5) δ = 21.1, 21.5, 87.3, 104.1, 110.0, 112.9, 115.7, 118.5, 121.1, 121.8, 122.1, 128.8, 129.1, 129.5, 132.6, 138.1, 140.0, 141.1, 141.6, 145.0, 145.8; IR (KBr) ν = 2944 (w), 2918 (s), 2850 (w), 2360 (w), 2343 (w), 1612 (w), 1577 (s), 1490 (s), 1428 (w), 1377 (w), 1336 (w), 1204 (s), 1099 (w), 1064 (w), 998 (s), 884 (w), 851 (s), 798 (s) cm^{-1}; ESI-MS: m/z (%) 964.8 (100) $[M + H]^+$. Anal. Calcd for $C_{64}H_{46}N_6Zn$: C, 79.70; H, 4.81; N, 8.71. Found: C, 79.33; H, 4.80; N, 8.87.

Complex 1. Compound **2** (2.05 mg, 1.23 μmol) and $Cu(CH_3CN)_4PF_6$ (0.917 mg, 2.46 μmol) were poured in a round-bottomed flask and dissolved in dry $CHCl_3$ and dry DCM. Then **3** (1.19 mg, 1.23 μmol) and DABCO (0.138 mg, 1.23 μmol) were added to the solution. After the solution was heated at 60 °C for 3 h, the solvent was removed, furnishing the complex in quantitative yield: mp > 300 °C; ^{1}H NMR (400 MHz, $CD_2Cl_2/CDCl_3$ 9:1) δ = −4.57 (s, 6 H, CH_2^{DABCO}), −4.54 (s, 6 H, CH_2^{DABCO}), 1.10 (s, 6 H, mes-CH_3), 1.11 (s, 6 H, mes-CH_3), 1.72 (s, 6 H, mes-CH_3), 1.77 (s, 6 H, mes-CH_3), 2.03 (s, 12 H, duryl-CH_3), 2.15 (s, 12 H, duryl-CH_3), 2.50 (s, 6 H, mes-CH_3), 2.58 (s, 12 H, mes-CH_3), 2.63 (s, 12 H, mes-CH_3), 6.49 (d, ^3J = 5.6 Hz, 4 H, d-H), 7.08 (d, ^3J = 5.6 Hz, 4 H, c-H), 7.13 (s, 4 H, 11-H), 7.32 (s, 4 H, f-H), 7.34 (s, 4 H, k-H), 7.57 (d, ^3J = 8.0 Hz, 4 H, [a or b]-H), 7.97 (d, ^3J = 8.0 Hz, 4 H, [b or a]-H), 8.00 (d, ^3J = 8.0 Hz, 4 H, [l or m]-H), 8.01 (d, ^3J = 8.0 Hz, 2 H, [4 or 7]-H), 8.02 (d, ^3J = 8.0 Hz, 2 H, [7 or 4]-H), 8.25 (s, 4 H, 5-, 6-H), 8.29 (d, ^3J = 8.0 Hz, 4 H, [m or l]-H), 8.37 (d, ^3J = 4.6 Hz, 4 H, β'-H), 8.38 (d, ^3J = 4.6 Hz, 4 H, β'-H), 8.56 (d, ^3J = 4.6 Hz, 4 H, β'-H), 8.57 (d, ^3J = 4.6 Hz, 4 H, β'-H), 8.78 (d, ^3J = 8.0 Hz, 2 H, [3 or 8]-H), 8.80 (d, ^3J = 8.0 Hz, 2 H, [8 or 3]-H); ^{13}C NMR (100 MHz, $CD_2Cl_2/CDCl_3$ 9:1) δ = 2.2 (C_{DABCO}), 18.4, 18.8, 20.8, 21.3, 21.5, 21.6, 22.5, 22.6, 27.3, 31.7, 39.4, 39.5, 87.1, 88.2, 98.4, 98.9, 116.9, 117.0, 118.0, 118.8, 119.2, 119.5, 120.6, 122.8, 125.5, 126.8, 127.6, 127.7, 127.8, 128.1, 128.6, 128.6, 129.2, 129.4, 130.5, 130.6, 130.9, 132.0, 132.1, 132.6, 134.5, 134.6, 134.9, 136.4, 137.7, 137.9, 138.0, 138.2, 138.9, 139.2, 139.7, 139.8, 140.0, 140.1, 140.2, 140.6, 143.7, 144.0, 144.2, 145.0, 148.8, 149.4, 149.6, 149.7, 150.6, 161.3, 161.6; IR (KBr) ν = 3445 (br, H_2O), 2975 (s), 2847 (s), 2306 (br), 2196 (br), 1604 (s), 1595 (s), 1422 (s), 1376 (w), 1340 (w), 1258 (s), 1224 (w), 1203 (w), 1153 (s), 1062 (w), 1030 (s), 850 (w), 797 (s) cm^{-1}; ESI-MS: m/z (%) 1435.0 (100) $[M - 2PF_6]^{2+}$. Anal. Calcd for $C_{186}H_{154}Cu_2F_{12}N_{16}P_2Zn_2 \cdot 2CH_2Cl_2 \cdot CH_3CN$: C, 67.68; H, 4.81; N, 7.06. Found: C, 67.57; H, 4.93; N, 7.40.

X-ray Crystal Structure Analysis. X-ray single-crystal diffraction data for compound **3** was collected on a SIEMENS SMART CCD diffractometer with Mo Kα radiation. The structure was solved using SHELXS-97 and refined by full-matrix least-squares analysis.[22] The hydrogen atoms were generated theoretically onto the specific atoms and refined isotropically with fixed thermal factors. The non-hydrogen atoms were refined with aniosotropic thermal parameters. There are disordered solvent molecules in the crystal lattice of the compounds, whose contribution to the structural data was removed by the SQUEEZE function.[23] Further details are provided in the Supporting Information.

Crystal data for 3: purple crystal; 0.70 × 0.32 × 0.22 mm; monoclinic; $P21/c$; a = 27.263 Å, b = 19.990 Å, c = 16.688 Å, β = 103.50°, V = 8842.35 Å^3; T = 164(2) K; Z = 4; ρ_{cal} = 1.416 g cm^{-3}; μ = 0.344 mm^{-1}; 70244 collected reflections, 9483 independent (R(int) = 0.256), GoF = 0.90, R1 = 0.0843, wR2 = 0.1712 for $I > 2\sigma(I)$ and R1 = 0.1918, wR2 = 0.1956 for all data.

Line Shape Analysis and Determination of Activation Barrier. The spectral simulations[19] were performed using the model of a two-spin system undergoing mutual exchange. Using the Eyring plot, activation of enthalpy ($\Delta H^{\ddagger}$) and activation of entropy ($\Delta S^{\ddagger}$) were determined from the slope and the intercept of the plot, respectively. Activation barrier ($\Delta G^{\ddagger}$) for the tumbling process at 298 K was determined using $\Delta G^{\ddagger} = \Delta H^{\ddagger} - T\Delta S^{\ddagger}$.

■ ASSOCIATED CONTENT

Supporting Information. ^{1}H NMR, ^{13}C NMR, ESI-MS, UV−vis, and DOSY for all relevant compounds and aggregates. This material is available free of charge via the Internet at http://pubs.acs.org.

■ AUTHOR INFORMATION

Corresponding Author
*E-mail: schmittel@chemie.uni-siegen.de.

■ ACKNOWLEDGMENT

Financial support by the Deutsche Forschungsgemeinschaft (Schm 647/15-1) and the University of Siegen is gratefully acknowledged.

■ REFERENCES

(1) (a) Von Delius, M.; Leigh, D. A. *Chem. Soc. Rev.* **2011**, *40*, 3656–3676. (b) Ma, X.; Tian, H. *Chem. Soc. Rev.* **2010**, *39*, 70. (c) Balzani, V.; Credi, A.; Venturi, M. *Molecular Devices and Machines*, 2nd ed.; Wiley-VCH: Weinheim, 2008. (d) Ballardini, R.; Balzani, V.; Credi, A.; Gandolfi, M. T.; Venturi, M. *Acc. Chem. Res.* **2001**, *34*, 445. (e) Urry, D. W. *Angew. Chem., Int. Ed.* **1993**, *32*, 819.

(2) (a) Fang, L.; Wang, C.; Fahrenbach, A. C.; Trabolsi, A.; Botros, Y. Y.; Stoddart, J. F. *Angew. Chem., Int. Ed.* **2011**, *50*, 1805. (b) Barrell, M. J.; Campana, A. G.; von Delius, M.; Geertsema, E. M.; Leigh, D. A. *Angew. Chem., Int. Ed.* **2011**, *50*, 285.(c) Silvi, S.; Venturi, M.; Credi, A. *Chem. Commun.* **2011**, *47*, 2483. (d) Carrol, G. T.; Pollard, M. M.; Delden, R. V.; Feringa, B. L. *Chem. Sci.* **2010**, *1*, 97. (e) Haberhauer, G. *Angew. Chem., Int. Ed.* **2010**, *49*, 9286. (f) Haberhauer, G.; Kallweit, C. *Angew. Chem., Int. Ed.* **2010**, *49*, 2418. (g) Balzani, V.; Credi, A.; Venturi, M. *Chem. Soc. Rev.* **2009**, *38*, 1542. (h) Kelly, R. T.; De Silva, H.; Silva, R. A. *Nature* **1999**, *401*, 150.

(3) (a) Barin, G.; Coskun, A.; Friedman, D. C.; Olson, M. A.; Colvin, M. T.; Carmielli, R.; Dey, S. K.; Bozdemir, O. A.; Wasielewski, M. R.; Stoddaart, J. F. *Chem.—Eur. J.* **2011**, *17*, 213. (b) Jiang, Y.; Guo, G.-B.; Chen, C.-F. *Org. Lett.* **2010**, *12*, 4248. (c) Busseron, E.; Romuald, C.; Coutrot, F. *Chem.—Eur. J.* **2010**, *16*, 10062. (d) Collin, J.-P.; Durola, F.; Lux, J.; Sauvage, J.-P. *Angew. Chem., Int. Ed.* **2009**, *48*, 8532. (e) Periyasamy, G.; Collin, J.-P.; Sauvage, J.-P.; Levine, R. D.; Remacle, F. *Chem.—Eur. J.* **2009**, *15*, 1310. (f) Coutrot, F.; Busseron, E. *Chem.—Eur. J.* **2009**, *15*, 5186. (g) Coutrot, F.; Romuald, C.; Busseron, E. *Org. lett.* **2008**, *10*, 3741. (h) Hirose, K.; Shiba, Y.; Ishibashi, K.; Doi, Y.; Tobe, Y. *Chem.—Eur. J.* **2008**, *14*, 3427.

(4) (a) Ruangsupapichat, N.; Pollard, M. M.; Harutyunyan, S. R.; Feringa, B. L. *Nature Chem.* **2011**, *3*, 53. (b) Ogi, S.; Ikeda, T.; Wakabayashi, R.; Shinkai, S.; Takeuchi, M. *Eur. J. Org. Chem.* **2011**, 1831. (c) Ogi, S.; Ikeda, T.; Wakabayashi, R.; Shinkai, S.; Takeuchi, M. *Chem.—Eur. J.* **2010**, *16*, 8285. (d) Otsuki, J.; Komatsu, Y.; Kobayashi, D.; Asakawa, M.; Miyake, K. *J. Am. Chem. Soc.* **2010**, *132*, 6870. (e) Moraoka, T.; Kinbara, K.; Aida, T. *Nature* **2006**, *440*, 512. (f) Koumura, N.; Zijlstra, R. W. J.; Van Delden, R. A.; Harada, N.; Feringa, B. L. *Nature* **1999**, *401*, 152.

(5) (a) Guenet, A.; Graf, E.; Kyritsakas, N.; Hosseini, M. W. *Chem.—Eur. J.* **2011**, *17*, 6443. (b) Lang, T.; Graf, E.; Kyritsakas, N.; Hosseini, M. W. *Dalton Trans.* **2011**, *40*, 3517. (c) Lang, T.; Guenet, A.; Graf, E.; Kyritsakas, N.; Hosseini, M. W. *Chem. Commun.* **2010**, *46*, 3508.

(d) Guenet, A.; Graf, E.; Kyritsakas, N.; Allouche, L.; Hosseini, M. W. *Chem. Commun.* **2007**, 2935.

(6) (a) Okuna, E.; Hiraoka, S.; Shionoya, M. *Dalton Trans.* **2010**, *39*, 4107. (b) Hiraoka, S.; Hisanaga, Y.; Shiro, M.; Shionoya, M. *Angew. Chem., Int. Ed.* **2010**, *49*, 1669. (c) Hiraoka, S.; Okuno, E.; Tanaka, T.; Shiro, M.; Shionoya, M. *J. Am. Chem. Soc.* **2008**, *130*, 9089. (d) Hiraoka, S.; Shiro, M.; Shionoya, M. *J. Am. Chem. Soc.* **2004**, *126*, 1214.

(7) Schmittel, M.; Samanta, S. K. *J. Org. Chem.* **2010**, *75*, 5911.

(8) (a) Rodriguez-Molina, B.; Farfan, N.; Romero, M.; Mendez-Stivalet, J. M.; Santillan, R.; Garcia-Garibay, M. A. *J. Am. Chem. Soc.* **2011**, *133*, 7280. (b) Yen, M.-L.; Chen, N.-C.; Lai, C.-C.; Liu, Y.-H.; Peng, S.-M.; Chiu, S.-H. *Dalton Trans.* **2011**, *40*, 2163. (c) Spruell, J. M.; Paxton, W. F.; Olsen, J.-C.; Benítez, D.; Tkatchouk, E.; Stern, C. L.; Trabolsi, A.; Friedman, D. C.; Goddard, W. A.; Stoddart, J. F. *J. Am. Chem. Soc.* **2009**, *131*, 11571. (d) Champin, B.; Mobian, P.; Sauvage, J.-P. *Chem. Soc. Rev.* **2007**, *36*, 358. (e) Liu, Y.; Flood, A. H.; Bonvallet, P. A.; Vignon, S. A.; Northrop, B. H.; Tseng, H.-R.; Jeppesen, J. O.; Huang, T. J.; Brough, B.; Baller, M.; Magonov, S.; Solares, S. D.; Goddard, W. A.; Ho, C.-M.; Stoddart, J. F. *J. Am. Chem. Soc.* **2005**, *127*, 9745. (f) Hiraoka, S.; Hirata, K.; Shionoya, M. *Angew. Chem., Int. Ed.* **2004**, *43*, 3814. (g) Comotti, A.; Bracco, S.; Valsesia, P.; Beretta, M.; Sozzani, P. *Angew. Chem., Int. Ed.* **2010**, *49*, 1760.

(9) (a) Nishimura, N.; Yoza, K.; Kobayashi *J. Am. Chem. Soc.* **2010**, *132*, 777. (b) Kitagawa, H.; Kobori, Y.; Yamanaka, M.; Yoza, K.; Kobayashi, K. *Proc. Natl. Acad. Sci. U.S.A.* **2009**, *106*, 10444. (c) Scarso, A.; Onagi, H.; Rebek, J., Jr. *J. Am. Chem. Soc.* **2004**, *126*, 12728. (d) Scarso., A.; Shivanyuk, A.; Hayashida, O.; Rebek, J., Jr. *J. Am. Chem. Soc.* **2003**, *125*, 6239.

(10) (a) Harthong, S.; Dubessy, B.; Vachon, J.; Aronica, C.; Mulatier, J.-C.; Dutasta, J.-P. *J. Am. Chem. Soc.* **2010**, *132*, 15637. (b) Mugridge, J. S.; Szigethy, G.; Bergman, R. G.; Raymond, K. N. *J. Am. Chem. Soc.* **2010**, *132*, 16256. (c) Hooley, R. J.; Van Anda, H. J.; Rebek, J., Jr. *J. Am. Chem. Soc.* **2007**, *129*, 13464.

(11) (a) Seo, W.; Phillips, S. T. *J. Am. Chem. Soc.* **2010**, *132*, 9234–9235. (b) Bassik, N.; Brafman, A.; Zarafshar, A. M.; Jamal, M.; Luvsanjav, D.; Selaru, F. M.; Gracias, D. H. *J. Am. Chem. Soc.* **2010**, *132*, 16314. (c) Leong, T. G.; Randall, C. L.; Benson, B. R.; Bassik, N.; Stern, G. M.; Gracias, D. H. *Proc. Natl. Acad. Sci. U.S.A.* **2009**, *106*, 703–708.

(12) Schmittel, M.; He, B.; Fan, J.; Bats, J. W.; Engeser, M.; Schlosser, M.; Deiseroth, H.-J. *Inorg. Chem.* **2009**, *48*, 8192.

(13) (a) Ballester, P.; Oliva, A. I.; Costa, A.; Deyà, P. M.; Frontera, A.; Gomila, R. M.; Hunter, C. A. *J. Am. Chem. Soc.* **2006**, *128*, 5560. (b) Baldini, L.; Ballester, P.; Casnati, A.; Gomila, R. M.; Hunter, C. A.; Sansone, F.; Ungaro, R. *J. Am. Chem. Soc.* **2003**, *125*, 14181.

(14) (a) Mahata, K.; Schmittel, M. *J. Am. Chem. Soc.* **2009**, *131*, 16544. (b) Schmittel, M.; He, B.; Mal, P. *Org. Lett.* **2008**, *10*, 2513. (c) Schmittel, M.; Kalsani, V.; Michel, C.; Mal, P.; Ammon, H.; Jäckel, F.; Rabe, J. P. *Chem.—Eur. J.* **2007**, *13*, 6223. (d) Schmittel, M.; Kalsani, V.; Kishore, R. S. K.; Cölfen, H.; Bats, J. W. *J. Am. Chem. Soc.* **2005**, *127*, 11545. (e) Schmittel, M.; Kalsani, V.; Bats, J. W. *Inorg. Chem.* **2005**, *44*, 4115.

(15) (a) Dry, E. F. V.; Clegg, J. K.; Breiner, B.; Whitaker, D. E.; Stefak, R.; Nitschke, J. R. *Chem. Commun.* **2011**, *47*, 6021. (b) Ohi, H.; Tachi, Y.; Itoh, S. *Inorg. Chem.* **2006**, *45*, 10825.

(16) Zhou, Z.; Cao, C.; Yin, Z.; Liu, C. *Org. Lett.* **2009**, *11*, 1781.

(17) (a) UV−vis titrations were analyzed by fitting the whole series of spectra at 0.5 nm intervals using the software SPECFIT. The SPECFIT program analyzes equilibrium data sets using singular value decomposition and linear regression modeling by the Levenberg−Marquardt method to determine cumulative binding constant. (b) Gampp, H.; Maeder, M.; Meyer, C. J.; Zuberbühler, A. D. *Talanta* **1985**, *32*, 257. (c) Gampp, H.; Maeder, M.; Meyer, C. J.; Zuberbühler, A. D. *Talanta* **1986**, *33*, 943.

(18) (a) Flamigni, L.; Talarico, A. M.; Ventura, B.; Rein, R.; Solladié, N. *Chem.—Eur. J.* **2006**, *12*, 701 and references cited therein. (b) Schuster, D. I.; Li, K.; Guldi, D. M.; Ramey, J. *Org. Lett.* **2004**, *6*, 1919. (c) Brettar, J.; Gisselbrecht, J.−P.; Gross, M.; Solladié, N. *Chem. Commun.* **2001**, 733.

(19) NMR Spectrum Calculations: WinDNMR, Version 7.1.13. Reich, H. J., Department of Chemistry, University of Wisconsin.

(20) Kishore, R. S. K.; Paululat, T.; Schmittel, M. *Chem.—Eur. J.* **2006**, *12*, 8136.

(21) Visser, J.; Katsonis, N.; Vicario, J.; Feringa, B. L. *Langmuir* **2009**, *25*, 5980.

(22) (a) Sheldrick, G. M. *SHELXS97: Program for Crystal Structure Determination*; University of Göttingen: Göttingen, Germany, 1997. (b) Sheldrick, G. M. *SHELXL97: Program for Crystal Structural Refinement*; University of Göttingen: Göttingen, Germany, 1997.

(23) (a) Spek, A. L. *Acta Crystallogr.* **1990**, *A46*, C34.(b) Spek, A. L. *PLATON, A Multipurpose Crystallographic Tool*; Ultrecht University: Ultrecht, The Netherlands, 2006.